

UNBIASED DEEP SOLVERS FOR LINEAR PARAMETRIC PDES

MARC SABATE VIDALES^{1,2}, DAVID ŠIŠKA^{2,3}, AND LUKASZ SZPRUCH^{1,2}

ABSTRACT. We develop several deep learning algorithms for approximating families of parametric PDE solutions. The proposed algorithms approximate solutions together with their gradients, which in the context of mathematical finance means that the derivative prices and hedging strategies are computed simultaneously. Having approximated the gradient of the solution one can combine it with a Monte-Carlo simulation to remove the bias in the deep network approximation of the PDE solution (derivative price). This is achieved by leveraging the Martingale Representation Theorem and combining the Monte Carlo simulation with the neural network. The resulting algorithm is robust with respect to quality of the neural network approximation and consequently can be used as a black-box in case only limited a priori information about the underlying problem is available. We believe this is important as neural network based algorithms often require fair amount of tuning to produce satisfactory results. The methods are empirically shown to work for high-dimensional problems (e.g. 100 dimensions). We provide diagnostics that shed light on appropriate network architectures.

1. INTRODUCTION

Numerical algorithms that solve PDEs suffer from the so-called “curse of dimensionality”, making it impractical to apply known discretisation algorithms such as finite differences schemes to solve high-dimensional PDEs. However, it has been recently shown that deep neural networks trained with stochastic gradient descent can overcome the curse of dimensionality [3, 6], making them a popular choice to solve this computational challenge in the last few years.

In this work, we focus on the problem of numerically solving parametric linear PDEs arising from European option pricing in high-dimensions. Let $B \subseteq \mathbb{R}^p$, $p \geq 1$ be a parameter space (for instance, in the Black–Scholes equation with fixed rate, B is the domain of the volatility parameter). Consider $v = v(t, x; \beta)$ satisfying

$$\begin{aligned} \left[\partial_t v + b \nabla_x v + \frac{1}{2} \text{tr} [\nabla_x^2 v \sigma^* \sigma] - cv \right] (t, x; \beta) &= 0, \\ v(T, x; \beta) &= g(x; \beta), \quad t \in [0, T], \quad x \in \mathbb{R}^d, \quad \beta \in B. \end{aligned} \quad (1)$$

Here $t \in [0, T]$, $x \in \mathbb{R}^d$ and $\beta \in B$ and b, σ, c and g are functions of $(t, x; \beta)$ which specify the problem. The Feynman–Kac theorem provides a probabilistic representation for v so that Monte Carlo methods can be used for its unbiased approximation in one single point $(t, x; \beta)$. What we propose in this work is a method for harnessing the power of deep learning algorithms to numerically solve (1) in a way that is robust even in edge cases when the output of the neural network is not of the expected quality, by combining them with Monte Carlo algorithms.

¹THE ALAN TURING INSTITUTE, ²UNIVERSITY OF EDINBURGH SCHOOL OF MATHEMATICS, ³VEGA
E-mail addresses: M.Sabate-Vidales@sms.ed.ac.uk, D.Siska@ed.ac.uk,
 L.Szpruch@ed.ac.uk.

Date: January 19, 2022.

2010 Mathematics Subject Classification. 65M75, 60H30, 91G60.

Key words and phrases. Monte Carlo method, Deep neural network, Control variates, Partial differential equations.

From the results in this article we observe that neural networks provide an efficient computational device for high dimensional problems. However, we observed that these algorithms are sensitive to the network architecture, parameters and distribution of training data. A fair amount of tuning is required to obtain good results. Based on this we believe that there is great potential in combining artificial neural networks with already developed and well understood probabilistic computational methods, in particular the control variate method for using potentially imperfect neural network approximations for finding unbiased solutions to a given problem, see Algorithm 1.

1.1. Main contributions. We propose three classes of learning algorithms for simultaneously finding solutions and gradients to parametric families of PDEs.

- i) *Projection solver*: See Algorithm 2. We leverage Feynman–Kac representation together with the fact that conditional expectation can be viewed as an L^2 -projection operator. The gradient can be obtained by automatic differentiation of already obtained approximation of the PDE solution.
- ii) *Martingale representation solver*: See Algorithm 3. This algorithm was inspired by Cvitanic et. al. [13] and Weinan et. al, Han et. al. [51, 22] and is referred to as deep BSDE solver. Our algorithm differs from [51] in that we approximate solution and its gradient at all the time-steps and across the entire space and parameter domains rather than only one space-time point. Furthermore we propose to approximate the solution-map and its gradient by separate networks.
- iii) *Martingale control variates solver*: Algorithms 4 and 5. Here we exploit the fact that martingale representation induces control variate that can produce zero variance estimator. Obviously, such control variate is not implementable but provides a basis for a novel learning algorithm for the PDE solution.

For each of these classes of algorithms we develop and test different implementation strategies. Indeed, one can either take one (large) network to approximate the entire family of solutions of (1) or take a number of (smaller) networks, where each of them approximates the solution at a time point in a grid. The former has the advantage that one can take arbitrarily fine time discretisation without increasing the overall network size. The advantage of the latter is that each learning task is simpler due to each network being smaller. One can further leverage the smoothness of the solution in time and learn the weights iteratively by initialising the network parameters to be those of the previous time step. We test both approaches numerically. At a high level all the algorithms work in path-dependent (non-Markovian) setting but there the challenge is an efficient method for encoding information in each path. This problem is solved in companion paper [45].

To summarise the key contribution of this work are:

- i) We derive and implement three classes of learning algorithms for approximation of parametric PDE solution map and its gradient.
- ii) We propose a novel iterative training algorithm that exploits regularity of the function we seek to approximate and allows using neural networks with smaller number of parameters.
- iii) The proposed algorithms are truly black-box in that quality of the network approximation only impacts the computation benefit of the approach and does not introduce approximation bias. This is achieved by combining the network approximation with Monte Carlo as stated in Algorithm 1.
- iv) Code for the numerical experiments presented in this paper is being made available on GitHub: <https://github.com/msabvid/Deep-PDE-Solvers>.

We stress the importance of point iii) above by directing reader’s attention to Figure 1, where we test generalisation error of trained neural network for the 5 dimensional family of PDEs corresponding to pricing a basket option under the Black–Scholes model. We refer reader to Example D.2 for details. We see that while the average error over test set

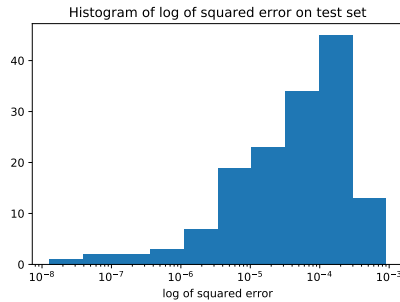


FIGURE 1. Histogram of mean-square-error of solution to the PDE on the test data set.

is of order $\approx 10^{-5}$, the errors for a given input varies significantly. Indeed, it has been observed in deep learning community that for high dimensional problems one can find input data such that trained neural network that appears to generalise well (i.e achieves small errors on the out of training data) produces poor results [19].

1.2. Literature review. Deep neural networks trained with stochastic gradient descent proved to be extremely successful in number of applications such as computer vision, natural language processing, generative models or reinforcement learning [36]. The application to PDE solvers is relatively new and has been pioneered by Weinan et. al, Han et. al. [51, 22, 47]. See also Cvitanic et. al. [13] for the ideas of solving PDEs with gradient methods and for direct PDE approximation algorithm. PDEs provide an excellent test bed for neural networks approximation because a) there exists alternative solvers e.g Monte Carlo b) we have well developed theory for PDEs, and that knowledge can be used to tune algorithms. This is contrast to mainstream neural networks approximations in text or images classification.

Apart from growing body of empirical results in literature on “Deep PDEs solvers”, [9, 28, 2, 31, 24] there has been also some important theoretical contributions. It has been proved that deep artificial neural networks approximate solutions to parabolic PDEs to an arbitrary accuracy without suffering from the curse of dimensionality. The first mathematically rigorous proofs are given in [20] and [32]. The high level idea is to show that neural network approximation to the PDE can be established by building on Feynman-Kac approximation and Monte-Carlo approximation. By checking that Monte-Carlo simulations do not suffer from the curse of dimensionality one can imply that the same is true for neural network approximation. Furthermore, it has been recently demonstrated in [27, 39] that noisy gradient descent algorithm used for training of neural networks of the form considered in [20, 32] induces unique probability distribution function over the parameter space which minimises learning. See [15, 10, 44, 48, 50, 23] for related ideas on convergence of gradient algorithms for overparametrised neural networks. This means that there are theoretical guarantees for the approximation of (parabolic) PDEs with neural networks trained by noisy gradient methods alleviating the curse of dimensionality.

An important application of deep PDE solvers is that one can in fact approximate a parametric family of solutions of a PDE. To be more precise let $B \subseteq \mathbb{R}^p$, $p \geq 1$, be a parameter space. In the context of finance these, for example, might be initial volatility, volatility of volatility, interest rate and mean reversion parameters. One can approximate the parametric family of functions $F(\cdot; \beta)_{\beta \in B}$ for an arbitrary range of parameters. This then allows for swift calibration of models to data (e.g options prices). This is particularly appealing for high dimensional problems when calibrating directly using noisy Monte-Carlo samples might be inefficient. This line of research gained some popularity recently and the idea has been tested numerically on various models and data sets [26, 37, 1, 49,

25, 30, 38]. There are some remarks that are in order. In the context of models calibration, while the training might be expensive one can do it offline, once and for good. One can also notice that training data could be used to produce a “look-up table” taking model parameters to prices. From this perspective the neural network, essentially, becomes an interpolator and a compression tool. Indeed the number of parameters of the network is much smaller than number of training data and therefore it is more efficient to store those. The final remark is that while there are other methods out there, such as Chebyshev functions, neural networks seem robust in high dimensions which make them our method of choice.

1.3. Notation. We denote by \mathcal{DN} the set of all fully connected feedforward neural networks (see Appendix C). We also use $\mathcal{R}[f]_\theta \in \mathcal{DN}$ with $\theta \in \mathbb{R}^\kappa$ to denote a neural network with weights θ approximating the function $f : \mathbb{R}^{d_0} \rightarrow \mathbb{R}^{d_1}$ for some $d_0, d_1 \in \mathbb{N}$.

1.4. Outline. This paper is organised as follows. Section 2 provides theoretical underpinning for the derivation of all the algorithms we propose to solve (1). More specifically in Section 2.2 we combine the approximation of the gradient of the solution of the PDE resulting from the Deep Learning algorithms with Monte Carlo to obtain an unbiased approximation of the solution of the PDE. In Section 3, we describe the algorithms in detail.

Finally in Section 4 we provide numerical tests of the proposed algorithms. We empirically test these methods on relevant examples including a 100 dimensional option pricing problems, see Examples 4.4 and D.3. We carefully measure the training cost and report the variance reduction achieved.

Since we work in situation where the function approximated by neural network can be obtained via other methods (Monte-Carlo, PDE solution) we are able to test the how the expressiveness of fully connected artificial neural networks depends on the number of layers and neurons per layer. See Section D.1 for details.

2. PDE MARTINGALE CONTROL VARIATE

Control variate is one of the most powerful variance reduction techniques for Monte-Carlo simulation. While a good control variate can reduce the computational cost of Monte-Carlo computation by several orders of magnitude, it relies on judiciously chosen control variate functions that are problem specific. For example, when computing price of basket options a sound strategy is to choose control variates to be call options written on each of the stocks in the basket, since in many models these are priced by closed-form formulae. In this article, we are interested in black-box-type control variate approach by leveraging the Martingale Representation Theorem and neural networks. The idea of using Martingale Representation to obtain control variates goes back at least to [41]. It has been further studied in combination with regression in [40] and [4].

The bias in the approximation of the solution can be completely removed by employing control variates where the deep network provides the control variate resulting in very high variance reduction factor in the corresponding Monte Carlo simulation.

Let $(\Omega, \mathcal{F}, \mathbb{P})$ be a probability space and consider an $\mathbb{R}^{d'}$ -valued Wiener process $W = (W^j)_{j=1}^{d'} = ((W_t^j)_{t \geq 0})_{j=1}^{d'}$. We will use $(\mathcal{F}_t^W)_{t \geq 0}$ to denote the filtration generated by W . Consider a $D \subseteq \mathbb{R}^d$ -valued, continuous, stochastic process defined for the parameters $\beta \in B \subseteq \mathbb{R}^p$, $X^\beta = (X^{\beta,i})_{i=1}^d = ((X_t^{\beta,i})_{t \geq 0})_{i=1}^d$ adapted to $(\mathcal{F}_t^W)_{t \geq 0}$ given as the solution to

$$dX_s^\beta = b(s, X_s^\beta; \beta) ds + \sigma(s, X_s; \beta) dW_s, \quad s \in [t, T], \quad X_t^\beta = x \in \mathbb{R}^d. \quad (2)$$

We will use $(\mathcal{F}_t^\beta)_{t \geq 0}$ to denote the filtration generated by X^β .

Let $g : \mathbb{R}^d \rightarrow \mathbb{R}$ be a measurable function and we assume that there is a (stochastic) discount factor given by

$$D(t_1, t_2; \beta) := e^{-\int_{t_1}^{t_2} c(s, X_s^\beta; \beta) ds}$$

for an appropriate function $c = c(t, x; \beta)$. We will omit β from the discount factor notation for brevity. We now interpret \mathbb{P} as some risk-neutral measure and so the \mathbb{P} -price of our contingent claim is

$$v(t, x; \beta) := \mathbb{E} \left[D(t, T) g(X_T^\beta) \middle| X_t^\beta = x \right]. \quad (3)$$

Say we have iid r.v.s $(X_T^{\beta, i})_{i=1}^N$ with the same distribution as X_T^β , where for each i , $X_t^{\beta, i} = x$. Then the standard Monte-Carlo estimator is

$$v^N(t, x; \beta) := \frac{1}{N} \sum_{i=1}^N D^i(t, T) g(X_T^{\beta, i}).$$

Convergence $v^N(t, x; \beta) \rightarrow v(t, x; \beta)$ in probability as $N \rightarrow \infty$ is granted by the Law of Large Numbers. Moreover the classical Central Limit Theorem tells that

$$\mathbb{P} \left(v(t, x; \beta) \in \left[v^N(t, x; \beta) - z_{\alpha/2} \frac{\sigma}{\sqrt{N}}, v^N(t, x; \beta) + z_{\alpha/2} \frac{\sigma}{\sqrt{N}} \right] \right) \rightarrow 1 - \alpha \text{ as } N \rightarrow \infty,$$

where $\sigma := \sqrt{\text{Var} [D(t, T) g(X_T^\beta)]}$ and $z_{\alpha/2}$ is such that $1 - \Phi(z_{\alpha/2}) = \alpha/2$ with Φ being distribution function (cumulative distribution function) of the standard normal distribution. To decrease the width of the confidence intervals one can increase N , but this also increases the computational cost. A better strategy is to reduce variance by finding an alternative Monte-Carlo estimator, say $\mathcal{V}^N(t, x; \beta)$, such that

$$\mathbb{E}[\mathcal{V}^N(t, x; \beta)] = v(t, x; \beta) \quad \text{and} \quad \text{Var}[\mathcal{V}^N(t, x; \beta)] < \text{Var}[v^N(t, x; \beta)], \quad (4)$$

and the cost of computing $\mathcal{V}^N(t, x; \beta)$ is similar to $v^N(t, x; \beta)$.

In the remainder of the article we will devise and test several strategies, based on deep learning, to find a suitable approximation for $\mathcal{V}^N(t, x; \beta)$, by exploring the connection of the SDE (2) and its associated PDE.

2.1. PDE derivation of the control variate. It can be shown that under suitable assumptions on b, σ, c and g , and fixed $\beta \in B$ that $v \in C^{1,2}([0, T] \times D)$. See e.g. [33]. Let $a := \frac{1}{2} \sigma \sigma^*$. Then, from Feynman–Kac formula (see e.g. Th. 8.2.1 in [42]), we get

$$\begin{cases} [\partial_t v + \text{tr}(a \partial_x^2 v) + b \partial_x v - cv](t, x; \beta) = 0 & \text{in } [0, T] \times D, \\ v(T, \cdot) = g & \text{on } D. \end{cases} \quad (5)$$

Since $v \in C^{1,2}([0, T] \times D)$ and since v satisfies the above PDE, if we apply Itô's formula then we obtain

$$D(t, T) v(T, X_T^\beta; \beta) = v(t, x; \beta) + \int_t^T D(t, s) \partial_x v(s, X_s^\beta; \beta) \sigma(s, X_s^\beta; \beta) dW_s. \quad (6)$$

Hence Feynman-Kac representation together with the fact that $v(T, X_T^\beta; \beta) = g(X_T^\beta)$ yields

$$v(t, x; \beta) = D(t, T) g(X_T^\beta) - \int_t^T D(t, s) \partial_x v(s, X_s^\beta; \beta) \sigma(s, X_s^\beta; \beta) dW_s. \quad (7)$$

Provided that

$$\sup_{s \in [t, T]} \mathbb{E}[|D(t, s) \partial_x v(s, X_s^\beta; \beta) \sigma(s, X_s^\beta; \beta)|^2] < \infty,$$

then the stochastic integral is a martingale. Thus we can consider the Monte-Carlo estimator.

$$\mathcal{V}^N(t, x; \beta) := \frac{1}{N} \sum_{i=1}^N \left\{ D^i(t, T)g(X_T^{\beta, i}) - \int_t^T D^i(t, s) \partial_x v(s, X_s^{\beta, i}; \beta) \sigma(s, X_s^{\beta, i}; \beta) dW_s^i \right\}. \quad (8)$$

To obtain a control variate we thus need to approximate $\partial_x v$. If one used classical approximation techniques to the PDE, such as finite difference or finite element methods, one would run into the curse of the dimensionality - the very reason one employs Monte-Carlo simulations in the first place. Artificial neural networks have been shown to break the curse of dimensionality in specific situations [20]. To be more precise, authors in [6, 16, 32, 21, 29, 20, 35, 18, 43] have shown that there always exist a deep feed forward neural network and some parameters such that the corresponding neural network can approximate the solution of a linear PDE arbitrarily well in a suitable norm under reasonable assumptions (terminal condition and coefficients can be approximated by neural networks). Moreover the number of parameters grows only polynomially in dimension and so there is no curse of dimensionality. However, while the papers above construct the network they do not tell us how to find the “good” parameters. In practice the parameter search still relies on gradient descent-based minimisation over a non-convex landscape. The application of the deep-network approximation to the solution of the PDE as a martingale control variate is an ideal compromise.

If there is no exact solution to the PDE (5), as would be the case in any reasonable application, then we will approximate $\partial_x v$ by $\mathcal{R}[\partial_x v]_\theta \in \mathcal{DN}$.

To obtain an implementable algorithm we discretise the integrals in $\mathcal{V}_t^{\beta, N, v}$ and take a partition of $[0, T]$ denoted $\pi := \{t = t_0 < \dots < t_{N_{\text{steps}}} = T\}$, and consider an approximation of (2) by $(X_{t_k}^{\beta, \pi})_{t_k \in \pi}$. For simplicity we approximate all integrals arising by Riemann sums always taking the left-hand point when approximating the value of the integrand.

The implementable control variate Monte-Carlo estimator is then the form

$$\begin{aligned} \mathcal{V}^{\pi, \theta, \lambda, N}(t, x; \beta) := & \frac{1}{N} \sum_{i=1}^N \left\{ (D^\pi(t, T))^i g(X_T^{\beta, \pi, i}) \right. \\ & \left. - \lambda \sum_{k=1}^{N_{\text{steps}}-1} (D^\pi(t, t_k))^i \mathcal{R}[\partial_x v]_\theta(t_k, X_{t_k}^{\beta, \pi, i}; \beta) \sigma(t_k, X_{t_k}^{\beta, \pi, i}; \beta) (W_{t_{k+1}}^i - W_{t_k}^i) \right\}, \end{aligned} \quad (9)$$

where $D^\pi(t, T) := e^{-\sum_{k=1}^{N_{\text{steps}}-1} c(t_k, X_{t_k}^{\beta, \pi})(t_{k+1} - t_k)}$ and λ is a free parameter to be chosen (because we discretise and use approximation to the PDE it is expected $\lambda \neq 1$). Again, we point out that the only bias of the above estimator comes from the numerical scheme used to solve the forward and backward processes. Nevertheless, $\mathcal{R}[\partial_x v]_\theta$ does not add any additional bias independently of the choice θ . We will discuss possible approximation strategies for approximating $\partial_x v$ with $\mathcal{R}[\partial_x v]_\theta$ in the following section.

In this section we have actually derived an explicit form of the Martingale representation (see e.g. [11, Th. 14.5.1]) of $D(t, T)g(X_T^\beta)$ in terms of the solution of the PDE associated to the process X^β , which is given as the solution to (2). In Appendix A we provide a more general framework to build a low-variance Monte Carlo estimator \mathcal{V}_t^N for any (possibly non-Markovian) \mathcal{F}^W -adapted process X^β .

2.2. Unbiased Parametric PDE approximation. After having trained the networks $\mathcal{R}[\partial_x v]_\theta$ (using any of Algorithms 2, 3, 4, 5 that we will introduce in Section 3) and $\mathcal{R}[v]_\eta$ (using any of Algorithms 2, 3) that approximate $v, \partial_x v$ one then has two options to approximate $v(t, x_t; \beta)$

- i) Directly with $\mathcal{R}[v]_\eta(t, x_t; \beta)$ if Algorithms 2 or 3 were used, which will introduce some approximation bias.

- ii) By combining $\mathcal{R}[\partial_x v]_\theta$ with the Monte Carlo approximation of $v(t, x_t; \beta)$ using (9), which will yield an unbiased estimator of $v(t, x_t; \beta)$. The complete method is stated as Algorithm 1.

Algorithm 1 Unbiased parametric PDE solver

Input: t, x, β where $t \in \pi$.

Initialisation: θ, N_{tm}

for $i : 1 : N_{\text{tm}}$ **do**

Generate samples $(x_t^{\beta, \pi, i})_{t \in \pi}$ by using numerical SDE solver on (2).

end for

Find the optimal weights $\theta^{*, N_{\text{tm}}}$ of $\mathcal{R}[\partial_x v]_\theta$ using one of Algorithms 2, 3, 4, 5.

return $\mathcal{V}_{t, T}^{\beta, \pi, \theta^*, \lambda, N}$ as defined in (9) with θ replaced by $\theta^{*, N_{\text{tm}}}$.

3. DEEP PDE SOLVERS

In this section we propose two algorithms that learn the PDE solution (or its gradient) and then use it to build control variate using (9). We also include in the Appendix B an additional algorithm to solve such linear PDEs using deep neural networks.

3.1. Projection solver. Before we proceed further we recall a well known property of conditional expectations, for proof see e.g. [34, Ch.3 Th. 14].

Theorem 3.1. *Let $\mathcal{X} \in L^2(\mathcal{F})$. Let $\mathcal{G} \subset \mathcal{F}$ be a sub σ -algebra. There exists a random variable $Y \in L^2(\mathcal{G})$ such that*

$$\mathbb{E}[|\mathcal{X} - \mathcal{Y}|^2] = \inf_{\eta \in L^2(\mathcal{G})} \mathbb{E}[|\mathcal{X} - \eta|^2].$$

The minimiser, \mathcal{Y} , is unique and is given by $\mathcal{Y} = \mathbb{E}[\mathcal{X}|\mathcal{G}]$.

The theorem tell us that conditional expectation is an orthogonal projection of a random variable X onto $L^2(\mathcal{G})$. Instead of working directly with (5) we work with its probabilistic representation (6). To formulate the learning task, we replace \mathcal{X} by $D(t, T)g((X_T^\beta))$ so that $v(t, X_t^\beta; \beta) = \mathbb{E}[\mathcal{X}|X_t^\beta]$. Hence, by Theorem (3.1),

$$\mathbb{E}[|\mathcal{X} - v(t, X_t^\beta; \beta)|^2] = \inf_{\eta \in L^2(\sigma(X_t^\beta))} \mathbb{E}[|\mathcal{X} - \eta|^2]$$

and we know that for a fixed t the random variable which minimises the mean square error is a function of X_t . But by the Doob–Dynkin Lemma [11, Th. 1.3.12] we know that every $\eta \in L^2(\sigma(X_t))$ can be expressed as $\eta = h_t(X_t^\beta)$ for some appropriate measurable h_t . For the practical algorithm we restrict the search for the function h_t to the class that can be expressed as deep neural networks \mathcal{DN} . Hence we consider a family of functions $\mathcal{R}_\theta \in \mathcal{DN}$ and set learning task as

$$\theta^* := \arg \min_{\theta} \mathbb{E}_{\beta} \left[\mathbb{E}_{(X_t^{\beta, \pi})_{t \in \pi}} \left[\sum_{k=0}^{N_{\text{steps}}} \left(D(t_k, T)g(X_T^{\beta, \pi}) - \mathcal{R}[v]_{\theta_{t_k}}(X_{t_k}^{\beta, \pi}; \beta) \right)^2 \right] \right]. \quad (10)$$

The inner expectation in (10) is taken across all paths generated using numerical scheme on (2) for a fixed β and it allows to solve the PDE (5) for such β . The outer expectation is taken on β for which the distribution is fixed beforehand (e.g. uniform on B if it is compact), thus allowing the algorithm to find the optimal neural network weights θ^* to solve the parametric family of PDEs (5). Automatic differentiation is used to approximate $\partial_x v$. Algorithm 2 describes the method.

Algorithm 2 Projection solver

Initialisation: θ , N_{trn} , distribution of β .

for $i : 1 : N_{\text{trn}}$ **do**

 generate samples $(x_t^{\beta, \pi, i})_{t \in \pi}$ by using numerical SDE solver on (2) and sampling from the distribution of β .

end for

Use SGD to find $\theta^{*, N_{\text{trn}}}$ where

$$\theta^{*, N_{\text{trn}}} = \arg \min_{\theta} \mathbb{E}^{\mathbb{P}^{N_{\text{trn}}}} \left[\sum_{k=0}^{N_{\text{steps}}-1} \left(D(t_k, T)g(X_T^{\beta, \pi}) - \mathcal{R}[v]_{\theta_{t_k}}(X_{t_k}^{\beta, \pi}; \beta) \right)^2 \right]$$

Where $\mathbb{E}^{\mathbb{P}^{N_{\text{trn}}}}$ denotes the empirical mean.

Automatic differentiation applied to $\mathcal{R}[v]_{\theta_{t_k}}(x_{t_k}^{\beta, \pi}; \beta)$ can be used to approximate $\partial_x v$.

return $\theta^{*, N_{\text{trn}}}$.

3.2. Probabilistic representation based on Backward SDE. Instead of working directly with (5) we work with its probabilistic representation (6) and view it as a BSDE. To formulate the learning task based on this we recall the time-grid π so that we can write it recursively as

$$\begin{aligned} v(t_{N_{\text{steps}}}, X_{t_{N_{\text{steps}}}}^{\beta}; \beta) &= g(X_{t_{N_{\text{steps}}}}^{\beta}), \\ D(t, t_{m+1})v(t_{m+1}, X_{t_{m+1}}^{\beta}; \beta) &= D(t, t_m)v(t_m, X_{t_m}^{\beta}; \beta) \\ &\quad + \int_{t_m}^{t_{m+1}} D(t, s)\partial_x v(s, X_s^{\beta}; \beta)\sigma(s, X_s^{\beta}; \beta) dW_s \text{ for } m = 0, 1, \dots, N_{\text{steps}} - 1. \end{aligned}$$

Next consider deep network approximations for each time step in π and for both the solution of (5) and its gradient.

$$\mathcal{R}[v]_{\eta_m}(x; \beta) \approx v(t_m, x; \beta), \quad t_m \in \pi, \quad x \in \mathbb{R}^d$$

and

$$\mathcal{R}[\partial_x v]_{\theta_m}(x; \beta) \approx \partial_x v(t_m, x; \beta), \quad t_m \in \pi, \quad x \in \mathbb{R}^d.$$

Approximation depends on weights $\eta_m \in \mathbb{R}^{k_\eta}$, $\theta_m \in \mathbb{R}^{k_\theta}$. We then set the learning task as

$$\begin{aligned} (\eta^*, \theta^*) &:= \arg \min_{(\eta, \theta)} \mathbb{E}_{\beta, X^\beta} \left[\left| g(X_{t_{N_{\text{steps}}}}^{\beta, \pi}) - \mathcal{R}[v]_{\eta_{N_{\text{steps}}}}(X_{t_{N_{\text{steps}}}}^{\beta, \pi}) \right|^2 \right. \\ &\quad \left. + \frac{1}{N_{\text{steps}}} \sum_{m=0}^{N_{\text{steps}}-1} |\mathcal{E}_{m+1}^{(\eta, \theta)}|^2 \right], \end{aligned} \quad (11)$$

$$\begin{aligned} \mathcal{E}_{m+1}^{(\eta, \theta)} &:= D(t, t_{m+1})\mathcal{R}[v]_{\eta_{m+1}}(X_{t_{m+1}}^{\beta, \pi}; \beta) - D(t, t_m)\mathcal{R}[v]_{\eta_m}(X_{t_m}^{\beta, \pi}; \beta) \\ &\quad - D(t, t_m)\mathcal{R}[\partial_x v]_{\theta_m}(X_{t_m}^{\beta, \pi}; \beta)\sigma(t_m, X_{t_m}^{\beta, \pi}; \beta)\Delta W_{t_{m+1}}, \end{aligned}$$

where

$$\eta = \{\eta_0, \dots, \eta_{t_{N_{\text{steps}}}}\}, \quad \theta = \{\theta_0, \dots, \theta_{t_{N_{\text{steps}}}}\}.$$

The complete learning method is stated as Algorithm 3, where we split the optimisation (11) in several optimisation problems, one per time step: learning the weights θ_m or η_m at a certain time step $t_m < t_{N_{\text{steps}}}$ only requires knowing the weights η_{m+1} . At $m = N_{\text{steps}}$, learning the weights $\eta_{N_{\text{steps}}}$ only requires the terminal condition g . Note that the algorithm assumes that adjacent networks in time will be similar, and therefore we initialise η_m and θ_m by η_{m+1}^* and θ_{m+1}^* .

Algorithm 3 Martingale representation solver, iterative

Initialisation: N_{trn}
for $i : 1 : N_{\text{trn}}$ **do**
 generate samples $(x_t^{\beta, \pi, i})_{t \in \pi}$ by using numerical SDE solver on (2) and sampling from the distribution of β .
end for

Initialisation: $\eta_{N_{\text{steps}}}$

Find $\eta_{N_{\text{steps}}}^{*, N_{\text{trn}}}$ using SGD where

$$\eta_{N_{\text{steps}}}^{*, N_{\text{trn}}} := \arg \min_{\eta} \frac{1}{N_{\text{trn}}} \sum_{i=1}^{N_{\text{trn}}} \left| g(x_{t_{N_{\text{steps}}}}^{\beta, \pi, i}) - \mathcal{R}[v]_{\eta_{N_{\text{steps}}}}(x_{t_{N_{\text{steps}}}}^{\beta, \pi, i}; \beta) \right|^2$$

for $m : N_{\text{steps}} - 1 : 0 : -1$ **do**

 Initialise $(\theta_m, \eta_m) = (\theta_{m+1}^{*, N_{\text{trn}}}, \eta_{m+1}^{*, N_{\text{trn}}})$

 Find $(\theta_m^{*, N_{\text{trn}}}, \eta_m^{*, N_{\text{trn}}})$ using SGD where

$$(\theta_m^{*, N_{\text{trn}}}, \eta_m^{*, N_{\text{trn}}}) := \arg \min_{(\eta_m, \theta_m)} \frac{1}{N_{\text{trn}}} \sum_{i=1}^{N_{\text{trn}}} \left| \mathcal{E}_{m+1}^{\beta, \pi, i, (\eta, \theta)} \right|^2$$

 where

$$\begin{aligned} \mathcal{E}_{m+1}^{\pi, i, (\eta, \theta)} := & D^{\pi, i}(t, t_{m+1}) \mathcal{R}[v]_{\eta_{m+1}}(x_{t_{m+1}}^{\beta, \pi, i}; \beta) - D^{\pi, i}(t, t_m) \mathcal{R}[v]_{\eta_m}(x_{t_m}^{\beta, \pi, i}; \beta) \\ & - D^{\pi, i}(t, t_m) \mathcal{R}[\partial_x v]_{\theta_m}(x_{t_m}^{\beta, \pi, i}; \beta) \sigma(t_m, x_{t_m}^{\beta, \pi, i}; \beta) \Delta W_{t_{m+1}}^i. \end{aligned}$$

end for

return $(\theta_m^{*, N_{\text{trn}}}, \eta_m^{*, N_{\text{trn}}})$ for all $m = 0, 1, \dots, N_{\text{steps}}$.

3.3. Martingale Control Variate deep solvers. So far, the presented methodology to obtain the control variate consists on first learning the solution of the PDE and more importantly its gradient (Algorithms 2, 3) which is then plugged in (9). Alternatively, one can directly use the variance of (9) as the loss function to be optimised in order to learn the control variate. We expand this idea and design two additional algorithms.

Recall definition of $\mathcal{V}_{t, T}^{\beta, \pi, \theta, \lambda, N}$ given by (9). From (8) we know that the theoretical control variate Monte-Carlo estimator has zero variance and so it is natural to set-up a learning task which aims to learn the network weights θ in a way which minimises said variance:

$$\theta^{*, \text{var}} := \arg \min_{\theta} \text{Var} \left[\mathcal{V}_{t, T}^{\beta, \pi, \theta, \lambda, N} \right].$$

Setting $\lambda = 1$, the learning task is stated as Algorithm 4.

Algorithm 4 Martingale control variates solver: Empirical variance minimisation

Initialisation: θ, N_{trn}

for $i : 1 : N_{\text{trn}}$ **do**

 generate samples $(x_t^{\beta, \pi, i})_{t \in \pi}$ by using numerical SDE solver on (2) and sampling from the distribution of β .

end for

Find $\theta^{*, N_{\text{trn}}}$ where

$$\theta^{*, N_{\text{trn}}} := \arg \min_{\theta} \text{Var}^{N_{\text{trn}}} \left[\mathcal{V}_{t, T}^{\beta, \pi, \theta, \lambda, N_{\text{trn}}} \right],$$

where $\text{Var}^{N_{\text{trn}}}$ denotes the empirical variance, and $\mathcal{V}_{t, T}^{\beta, \pi, \theta, \lambda, N}$ is obtained from (9).

return $\theta^{*, N_{\text{trn}}}$.

We include a second similar Algorithm in Appendix B.

4. EXAMPLES AND EXPERIMENTS

4.1. Options in Black–Scholes model on $d > 1$ assets. Take a d -dimensional Wiener process W . We assume that we are given a symmetric, positive-definite matrix (covariance matrix) Σ and a lower triangular matrix C s.t. $\Sigma = CC^*$. For such a positive-definite Σ we can always use Cholesky decomposition to find C . The risky assets will have volatilities given by σ^i . We will (abusing notation) write $\sigma^{ij} := \sigma^i C^{ij}$, when we don't need to separate the volatility of a single asset from correlations. The risky assets under the risk-neutral measure are then given by

$$dS_t^i = rS_t^i dt + \sigma^i S_t^i \sum_j C^{ij} dW_t^j. \quad (12)$$

All sums will be from 1 to d unless indicated otherwise. Note that the SDE can be simulated exactly since

$$S_{t_{n+1}}^i = S_{t_n}^i \exp \left(\left(r - \frac{1}{2} \sum_j (\sigma^{ij})^2 \right) (t_{n+1} - t_n) + \sum_j \sigma^{ij} (W_{t_{n+1}}^j - W_{t_n}^j) \right).$$

The associated PDE is (with $a^{ij} := \sum_k \sigma^{ik} \sigma^{jk}$)

$$\partial_t v(t, S) + \frac{1}{2} \sum_{i,j} a^{ij} S^i S^j \partial_{x_i x_j} v(t, S) + r \sum_i S^i \partial_{S^i} v(t, S) - rv(t, S) = 0,$$

for $(t, S) \in [0, T) \times (\mathbb{R}^+)^d$ together with the terminal condition $v(T, S) = g(S)$ for $S \in (\mathbb{R}^+)^d$.

4.2. Deep Learning setting. In this subsection we describe the neural networks used in the four proposed algorithms as well as the training setting, in the specific situation where we have an options problem in Black-Scholes model on $d > 1$ assets.

Learning algorithms 3, 4 and 5 share the same underlying fully connected artificial neural network which will be different for different $t_k, k = 0, 1, \dots, N_{\text{steps}} - 1$. At each time-step we use a fully connected artificial neural network denoted $\mathcal{R}[\cdot]_{\theta_k} \in \mathcal{DN}$. The choice of the number of layers and network width is motivated by empirical results on different possible architectures applied on a short-lived options problem. We present the results of this study in Appendix D.1. The architecture is similar to that proposed in [2].

At each time step the network consists of four layers: one d -dimensional input layer, two $(d + 20)$ -dimensional hidden layers, and one output layer. The output layer is one dimensional if the network is approximation for v and d -dimensional if the network is an approximation for $\partial_x v$. The non-linear activation function used on the hidden layers is the linear rectifier `relu`. In all experiments except for Algorithm 3 for the basket options problem we used batch normalisation [46] on the input of each network, just before the two nonlinear activation functions in front of the hidden layers, and also after the last linear transformation.

The networks' optimal parameters are approximated by the Adam optimiser [14] on the loss function specific for each method. Each parameter update (i.e. one step of the optimiser) is calculated on a batch of $5 \cdot 10^3$ paths $(x_{t_n}^i)_{n=0}^{N_{\text{steps}}}$ obtained by simulating the SDE. We take the necessary number of training steps until the stopping criteria defined below is met, with a learning rate of 10^{-3} during the first 10^4 iterations, decreased to 10^{-4} afterwards.

During training of any of the algorithms, the loss value at each iteration is kept. A model is assumed to be trained if the difference between the loss averages of the two last consecutive windows of length 100 is less than a certain ϵ .

4.3. Evaluating variance reduction. We use the specified network architectures to assess the variance reduction in several examples below. After training the models in each particular example, they are evaluated as follows:

- i) We calculate $N_{\text{MC}} = 10$ times the Monte Carlo estimate $\overline{\Xi}_T := \frac{1}{N_{\text{in}}} \sum_{i=1}^{N_{\text{in}}} \Xi_T^i$ and the Monte Carlo with control variate estimate $\bar{\mathcal{V}}_{t,T}^{\pi,\theta,\lambda,N_{\text{steps}}} = \frac{1}{N_{\text{in}}} \sum_{i=1}^{N_{\text{in}}} \mathcal{V}_{t,T}^{\pi,\theta,\lambda,N_{\text{steps}},i}$ using $N_{\text{in}} = 10^6$ Monte Carlo samples.
- ii) From Central Limit Theorem, as N_{in} increases the standardised estimators converge in distribution to the Normal. Therefore, a 95% confidence interval of the variance of the estimator is given by

$$\left[\frac{(N_{\text{MC}} - 1)S^2}{\chi_{1-\alpha/2, N_{\text{MC}}-1}}, \frac{(N_{\text{MC}} - 1)S^2}{\chi_{\alpha/2, N_{\text{MC}}-1}} \right]$$

where S is the sample variance of the N_{MC} controlled estimators $\bar{\mathcal{V}}_{t,T}^{\pi,\theta,\lambda,N_{\text{steps}}}$, and $\alpha = 0.05$. These are calculated for both the Monte Carlo estimate and the Monte Carlo with control variate estimate.

- iii) We use the $N_{\text{MC}} \cdot N_{\text{in}} = 10^7$ generated samples Ξ_T^i and $\mathcal{V}_{t,T}^{\pi,\theta,\lambda,N_{\text{steps}},i}$ to calculate and compare the empirical variances $\tilde{\sigma}_{\Xi_T}^2$ and $\tilde{\sigma}_{\mathcal{V}_{t,T}^{\pi,\theta,\lambda,N_{\text{steps}},i}}^2$.
- iv) The number of optimizer steps and equivalently number of random paths generated for training provide a cost measure of the proposed algorithms.
- v) We evaluate the variance reduction if we use the trained models to create control variates for options in Black-Scholes models with different volatilities than the one used to train our models.

Example 4.1 (Low dimensional problem with explicit solution). We consider exchange option on two assets. In this case the exact price is given by the Margrabe formula. We take $d = 2$, $S_0^i = 100$, $r = 5\%$, $\sigma^i = 30\%$, $\Sigma^{ii} = 1$, $\Sigma^{ij} = 0$ for $i \neq j$. The payoff is

$$g(S) = g(S^{(1)}, S^{(2)}) := \max\left(0, S^{(1)} - S^{(2)}\right).$$

From Margrabe's formula we know that

$$v(0, S) = \text{BlackScholes}\left(\text{risky price} = \frac{S^{(1)}}{S^{(2)}}, \text{strike} = 1, T, r, \bar{\sigma}\right),$$

where $\bar{\sigma} := \sqrt{(\sigma^{11} - \sigma^{21})^2 + (\sigma^{22} - \sigma^{12})^2}$.

We organise the experiment as follows: We train our models with batches of 5,000 random paths $(s_{t_n}^i)_{n=0}^{N_{\text{steps}}}$ sampled from the SDE 12, where $N_{\text{steps}} = 50$. The assets' initial values $s_{t_0}^i$ are sampled from a lognormal distribution

$$X \sim \exp((\mu - 0.5\sigma^2)\tau + \sigma\sqrt{\tau}\xi),$$

where $\xi \sim \mathcal{N}(0, 1)$, $\mu = 0.08$, $\tau = 0.1$. The existence of an explicit solution allows to build a control variate of the form (9) using the known exact solution to obtain $\partial_x v$. For a fixed number of time steps N_{steps} this provides an upper bound on the variance reduction an artificial neural network approximation of $\partial_x v$ can achieve.

We follow the evaluation framework to evaluate the model, simulating $N_{\text{MC}} \cdot N_{\text{in}}$ paths by simulating (12) with constant $(S_0^1, S_0^2)^i = (1, 1)$. We report the following results:

- i) Table 1 provides the empirical variances calculated over 10^6 generated Monte Carlo samples and their corresponding control variates. The variance reduction measure indicates the quality of each control variate method. The variance reduction using the control variate given by Margrabe's formula provides a benchmark for our methods. Table 1 also provides the cost of training for each method, given by the number of optimiser iterations performed before hitting the stopping criteria, defined before with $\epsilon = 5 \times 10^{-6}$. We add an additional row with the control variate built

using automatic differentiation on the network parametrised using the Deep Galerkin Method [47]. The DGM attempts to find the optimal parameters of the network satisfying the PDE on a pre-determined time and space domain. In contrast to our algorithms, the DGM method is not restricted to learn the solution of the PDE on the paths built from the probabilistic representation of the PDE. However, this is what is precisely enhancing the performance of our methods in terms of variance reduction, since they are specifically learning an approximation to the solution of the PDE and its gradient such that the resulting control variate will yield a low-variance Monte Carlo estimator.

- ii) Table 2 provides the confidence intervals for the variances and of the Monte Carlo estimator, and the Monte Carlo estimator with control variate assuming these are calculated on 10^6 random paths. Moreover, we add the confidence interval of the variance of the Monte Carlo estimator calculated over N_{in} antithetic paths where the first $N_{in}/2$ Brownian paths generated using $(Z_i)_{i=1, \dots, N_{steps}}$ samples from a normal and the second half of the Brownian paths are generated using the antithetic samples $(-Z_i)_{i=1, \dots, N_{steps}}$. See [5, Section 4.2] for more details. All the proposed algorithms in this paper outperform the Monte Carlo estimator and the Monte Carlo estimator with antithetic paths; compared to the latter, our algorithms produce unbiased estimators with variances that two orders of magnitude less.
- iii) Figure 2 studies the iterative training for the BSDE solver. As it has been observed before, this type of training does not allow us to study the overall loss function as the number of training steps increases. Therefore we train the same model four times for different values of ϵ between 0.01 and 5×10^{-6} and we study the number of iterations necessary to meet the stopping criteria defined by ϵ , the variance reduction once the stopping criteria is met, and the relationship between the number of iterations and the variance reduction. Note that the variance reduction stabilises for $\epsilon < 10^{-5}$. Moreover, the number of iterations necessary to meet the stopping criteria increases exponentially as ϵ decreases, and therefore for our results printed in Tables 1 and 2 we employ $\epsilon = 5 \times 10^{-6}$.
- iv) Figure 4 displays the variance reduction after using the trained models on several Black Scholes problem with exchange options but with values of σ other than 0.3 which was the one used for training. We see that the various algorithms work similarly well in this case (not taking training cost into account). We note that the variance reduction is close to the theoretical maximum which is restricted by time discretisation. Finally we see that the variance reduction is still significant even when the neural network was trained with different model parameter (in our case volatility in the option pricing example). The labels of Figure 4 can be read as follows:
 - i) *MC + CV Corr op*: Monte-Carlo estimate with Deep Learning-based Control Variate built using Algorithm 5.
 - ii) *MC + CV Var op*: Monte-Carlo estimate with Deep Learning-based Control Variate built using Algorithm 4.
 - iii) *MC + CV BSDE solver*: Monte-Carlo estimate with Deep Learning-based Control Variate built using Algorithm 3.
 - iv) *MC + CV Margrabe*: Monte-Carlo estimate with Control Variate using analytical solution for this problem given by Margrabe formula.

Method	Emp. Var.	Var. Red. Fact.	Train. Paths	Opt. Steps
Monte Carlo	3.16×10^{-2}	-	-	-
Algorithm 2	2.47×10^{-4}	127.7	38×10^6	7 600
Algorithm 3	2.59×10^{-4}	121.98	6.945×10^6	1380
Algorithm 4	2.39×10^{-4}	132.28	36.055×10^6	7211
Algorithm 5	2.40×10^{-4}	131.53	45.61×10^6	9122
MC + CV Margrabe	2.12×10^{-4}	149.19	-	-
MC + CV DGM [47]	1.22×10^{-3}	25.8	-	-

TABLE 1. Results on exchange option problem on two assets, Example 4.1. Empirical Variance and variance reduction factor

Method	Confidence Interval Variance	Confidence Interval Estimator
Monte Carlo	$[2.36 \times 10^{-6}, 4.15 \times 10^{-6}]$	[0.1187, 0.1195]
Monte Carlo + antithetic paths	$[1.15 \times 10^{-6}, 2.02 \times 10^{-6}]$	[0.1191, 0.1195]
Algorithm 2	$[4.13 \times 10^{-9}, 1.09 \times 10^{-8}]$	[0.11919, 0.11926]
Algorithm 3	$[4.12 \times 10^{-9}, 1.09 \times 10^{-8}]$	[0.11919, 0.11925]
Algorithm 4	$[4.32 \times 10^{-9}, 1.14 \times 10^{-8}]$	[0.11919, 0.11926]
Algorithm 5	$[2.30 \times 10^{-9}, 6.12 \times 10^{-8}]$	[0.11920, 0.11924]
MC + CV Margrabe	$[3.10 \times 10^{-9}, 8.23 \times 10^{-9}]$	[0.11919, 0.11925]
MC + CV DGM [47]	$[3.10 \times 10^{-9}, 8.23 \times 10^{-9}]$	[0.11919, 0.11925]

TABLE 2. Results on exchange option problem on two assets, Example 4.1.

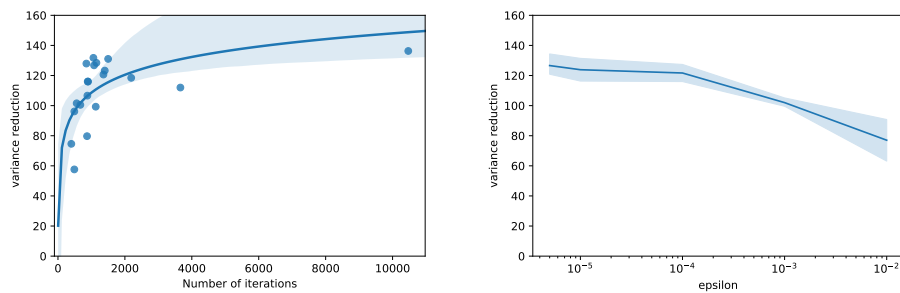


FIGURE 2. Left: Variance reduction in terms of number of optimiser iterations. Right: Variance reduction in terms of epsilon. Both are for Example 4.1 and Algorithm 3.

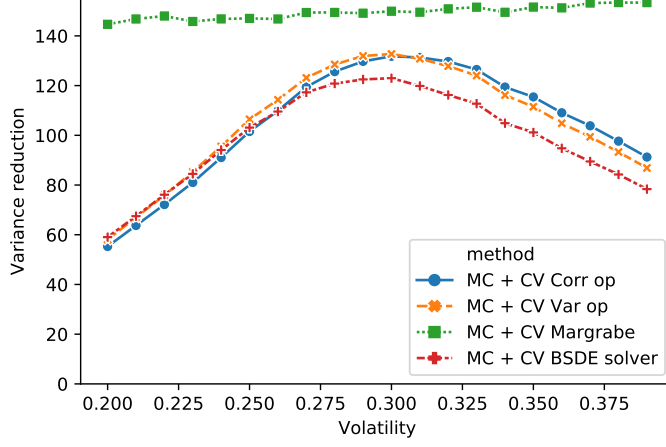


FIGURE 4. Variance reduction achieved by network trained with $\sigma = 0.3$ but then applied in situations where $\sigma \in [0.2, 0.4]$. We can see that the significant variance reduction is achieved by a neural network that was trained with “incorrect” σ . Note that the “MC + CV Margrabe” displays the optimal variance reduction that can be achieved by using exact solution to the problem. The variance reduction is not infinite even in this case since stochastic integrals are approximated by Riemann sums.

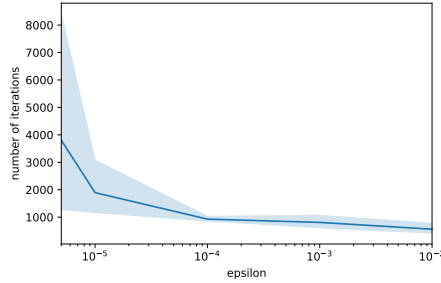


FIGURE 3. Number of optimiser iterations in terms of epsilon for Example 4.1 and Algorithm 3.

Example 4.2 (Low-dimensional problem with explicit solution - Approximation of Price using PDE solver compared to Control Variate). We consider exchange options on two assets as in Example 4.1. We consider algorithm 3 that can be applied in two different ways:

- i) It directly approximates the solution of the PDE (5) and its gradient in every point.
- ii) We can use $\partial_x v$ to build the control variate using probabilistic representation of the PDE (6)

We compare both applications by calculating the expected error of the L^2 -error of each of them with respect to the analytical solution given by Margrabe formula. From Margrabe’s formula we know that

$$v(0, S) = \text{BlackScholes} \left(\text{risky price} = \frac{S^{(1)}}{S^{(2)}}, \text{strike} = 1, T, r, \bar{\sigma} \right),$$

Let $\mathcal{R}[v]_{\eta_0}(x) \approx v(0, x)$ be the Deep Learning approximation of price at any point at initial time, calculated using Algorithm 3, and $\mathcal{R}[\partial_x v]_{\theta_m}(x) \approx \partial_x v(t_m, x)$ be the Deep Learning approximation of its gradient for every time step in the time discretisation. The aim of this experiment is to show how even if Algorithm 3 numerically converges to a biased approximation of $v(0, x)$ (see Figure 5 left), it is still possible to use $\mathcal{R}[\partial_x v]_{\theta_m}(x)$ to build an unbiased Monte-Carlo approximation of $v(0, x)$ with low variance.

We organise the experiment as follows.

- i) We calculate the expected value of the L^2 -error of $\mathcal{R}\eta_0(x)$ where each component of $x \in \mathbb{R}^2$ is sampled from a lognormal distribution:

$$\mathbb{E}[|v(0, x) - \mathcal{R}[v]_{\eta_0}(x)|^2] \approx \frac{1}{N} \sum_{i=1}^N |v(0, x^i) - \mathcal{R}[v]_{\eta_0}(x^i)|^2$$

- ii) We calculate the expected value of the L^2 -error of the Monte-Carlo estimator with control variate where each component of $x \in \mathbb{R}^2$ is sampled from a lognormal distribution:

$$\mathbb{E}[|v(0, x) - \mathcal{V}_{0,T}^{\pi, \theta, \lambda, N_{MC}, x}|^2] \approx \frac{1}{N} \sum_{i=1}^N |v(0, x^i) - \mathcal{V}_{0,T}^{\pi, \theta, \lambda, N_{MC}, x^i}|^2,$$

where $\mathcal{V}_{0,T}^{\pi, \theta, \lambda, N_{MC}, x}$ is given by 9, and is calculated for different values of Monte Carlo samples.

- iii) We calculate the expected value of the L^2 -error of the Monte-Carlo estimator without control variate where each component of $x \in \mathbb{R}^2$ is sampled from a lognormal distribution:

$$\mathbb{E}[|v(0, x) - \Xi_{0,T}^{\pi, \theta, \lambda, N_{MC}, x}|^2] \approx \frac{1}{N} \sum_{i=1}^N |v(0, x^i) - \Xi_{0,T}^{\pi, \theta, \lambda, N_{MC}, x^i}|^2,$$

where

$$\Xi_{0,T}^{\pi, \theta, \lambda, N_{MC}, x} := \frac{1}{N_{MC}} \sum_{j=1}^{N_{MC}} D(t, T) g(X_T^j)$$

Figure 5 provides one realisation of the described experiment for different Monte-Carlo iterations between 10 and 200. It shows how in this realisation, 60 Monte-Carlo iterations are enough to build a Monte-Carlo estimator with control variate having lower bias than the solution provided by Algorithm 3.

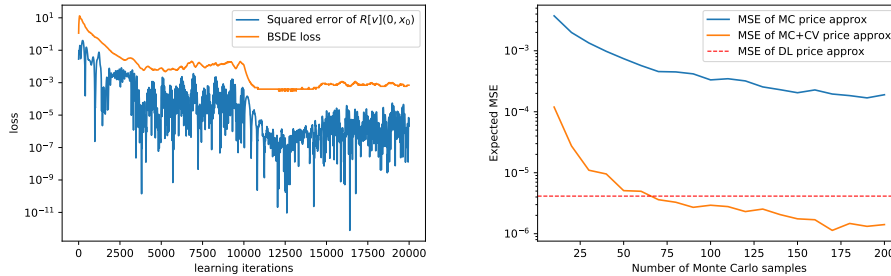


FIGURE 5. Left: Loss of Algorithm 3 and squared error of $\mathcal{R}[v](t, x_0)$ in terms of training iterations. Right: Expected MSE of the two different approaches with respect to analytical solution in terms of number of Monte Carlo samples

Example 4.3 (Low-dimensional problem with explicit solution. Training on random values for volatility). We consider exchange option on two assets. In this case the exact price is given by the Margrabe formula. The difference with respect to the last example is that now we aim to generalise our model, so that it can build control variates for different Black-Scholes models. For this we take $d = 2$, $S_0^i = 100$, $r = 0.05$, $\sigma^i \sim \text{Unif}(0.2, 0.4)$, $\Sigma^{ii} = 1$, $\Sigma^{ij} = 0$ for $i \neq j$.

The payoff is

$$g(S) = g(S^{(1)}, S^{(2)}) := \max\left(0, S^{(1)} - S^{(2)}\right).$$

We organise the experiment as follows: for comparison purposes with the BSDE solver from the previous example, we train our model for exactly the same number of iterations, i.e. 1,380 batches of 5,000 random paths $(s_{t_n}^i)_{n=0}^{N_{\text{steps}}}$ sampled from the SDE 12, where $N_{\text{steps}} = 50$. The assets' initial values $s_{t_0}^i$ are sampled from a lognormal distribution

$$X \sim \exp((\mu - 0.5\sigma^2)\tau + \sigma\sqrt{\tau}\xi),$$

where $\xi \sim \mathcal{N}(0, 1)$, $\mu = 0.08$, $\tau = 0.1$. Since now σ can take different values, it is included as input to the networks at each time step.

The existence of an explicit solution allows to build a control variate of the form (9) using the known exact solution to obtain $\partial_x v$. For a fixed number of time steps N_{steps} this provides an upper bound on the variance reduction an artificial neural network approximation of $\partial_x v$ can achieve.

Figure 6 adds the performance of this model to Figure 4, where the variance reduction of the Control Variate is displayed for different values of the volatility between 0.2 and 0.4.

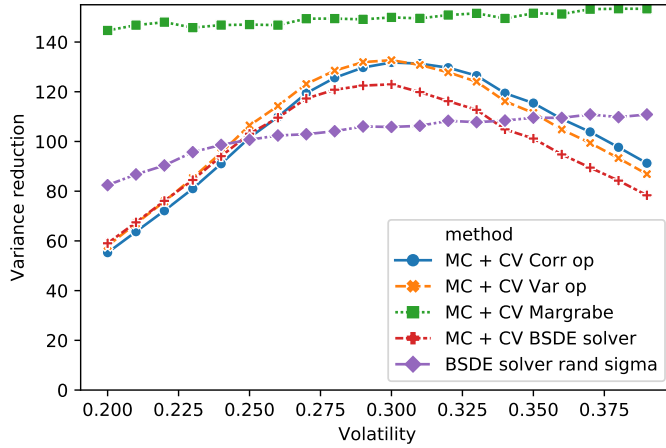


FIGURE 6. Extension of Figure 4 with variance reduction achieved by training the model on different Black-Scholes models

Example 4.4 (High-dimensional problem, exchange against average). We extend the previous example to 100 dimensions. This example is similar to EX_{10E} from [8]. We will take $S_0^i = 100$, $r = 5\%$, $\sigma^i = 30\%$, $\Sigma^{ii} = 1$, $\Sigma^{ij} = 0$ for $i \neq j$.

We will take this to be

$$g(S) := \max\left(0, S^1 - \frac{1}{d-1} \sum_{i=2}^d S^i\right).$$

The experiment is organised as follows: we train our models with batches of $5 \cdot 10^3$ random paths $(s_{t_n}^i)_{n=0}^{N_{\text{steps}}}$ sampled from the SDE (12), where $N_{\text{steps}} = 50$. The assets' initial values $s_{t_0}^i$ are sampled from a lognormal distribution

$$X \sim \exp((\mu - 0.5\sigma^2)\tau + \sigma\sqrt{\tau}\xi),$$

where $\xi \sim N(0, 1)$, $\mu = 0.08$, $\tau = 0.1$.

We follow the evaluation framework to evaluate the model, simulating $N_{\text{MC}} \cdot N_{\text{in}}$ paths by simulating (12) with constant $S_0^i = 1$ for $i = 1, \dots, 100$. We have the following results:

- i) Table 3 provides the empirical variances calculated over 10^6 generated Monte Carlo samples and their corresponding control variates. The variance reduction measure indicates the quality of each control variate method. Table 3 also provides the cost of training for each method, given by the number of optimiser iterations performed before hitting the stopping criteria with $\epsilon = 5 \cdot 10^{-6}$. Algorithm 3 outperforms the other algorithms in terms of variance reduction factor. This is not surprising as Algorithm 3 explicitly learns the discretisation of the Martingale representation (equation (7)) from which the control variate arises.
- ii) Table 4 provides the confidence interval for the variance of the Monte Carlo estimator, and the Monte Carlo estimator with control variate assuming these are calculated on 10^6 random paths.
- iii) Figures 7 and 8 study the iterative training for the BSDE solver. We train the same model four times for different values of ϵ between 0.01 and 5×10^{-6} and we study the number of iterations necessary to meet the stopping criteria defined by ϵ , the variance reduction once the stopping criteria is met, and the relationship between the number of iterations and the variance reduction. Note that in this case the variance reduction does not stabilise for $\epsilon < 10^{-5}$. However, the number of training iterations increases exponentially as ϵ decreases, and therefore we also choose $\epsilon = 5 \times 10^{-6}$ to avoid building a control that requires a high number of random paths to be trained.

Method	Emp. Var.	Var. Red. Fact.	Train. Paths	Opt. Steps
Monte Carlo	1.97×10^{-2}	-	-	-
Algorithm 2	5.94×10^{-3}	33.16	74×10^6	14 900
Algorithm 3	1.51×10^{-4}	130.39	14.145×10^6	2 829
Algorithm 4	5.29×10^{-4}	37.22	97.265×10^6	19 453
Algorithm 5	1.93×10^{-4}	102.05	76.03×10^6	15 206

TABLE 3. Results on exchange option problem on 100 assets, Example 4.4. Empirical Variance and variance reduction factor and costs in terms of paths used for training and optimizer steps.

Method	Confidence Interval Variance	Confidence Interval Estimator
Monte Carlo	$[1.51 \times 10^{-6}, 2.65 \times 10^{-6}]$	[0.0845, 0.0849]
Monte Carlo + antithetic paths	$[8.77 \times 10^{-7}, 1.53 \times 10^{-6}]$	[0.0845, 0.0848]
Algorithm 2	$[3.04 \times 10^{-8}, 2.14 \times 10^{-7}]$	[0.0848, 0.08493]
Algorithm 3	$[5.32 \times 10^{-9}, 1.41 \times 10^{-8}]$	[0.08485, 0.8492]
Algorithm 4	$[4.13 \times 10^{-9}, 1.09 \times 10^{-8}]$	[0.08484, 0.08490]
Algorithm 5	$[3.80 \times 10^{-9}, 1.0 \times 10^{-8}]$	[0.08487, 0.08493]

TABLE 4. Results on exchange option problem on 100 assets, Example 4.4.

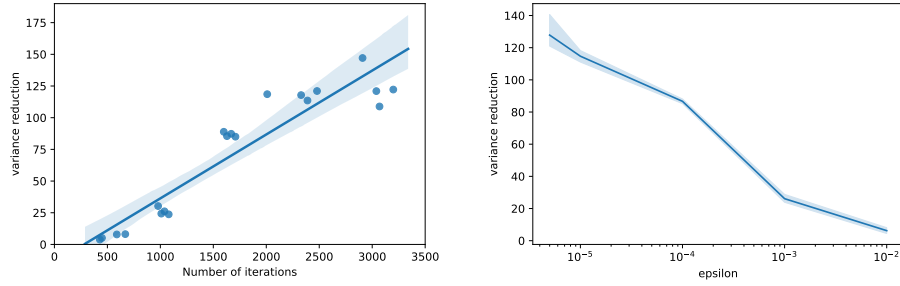


FIGURE 7. Left: Variance reduction in terms of number of optimiser iterations. Right: Variance reduction in terms of epsilon. Both for Example 4.4 and Algorithm 3.

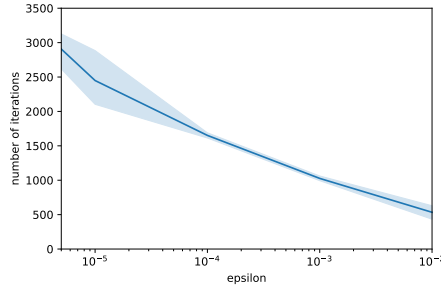


FIGURE 8. Number of optimiser iterations in terms of ϵ for Example 4.4 and Algorithm 3.

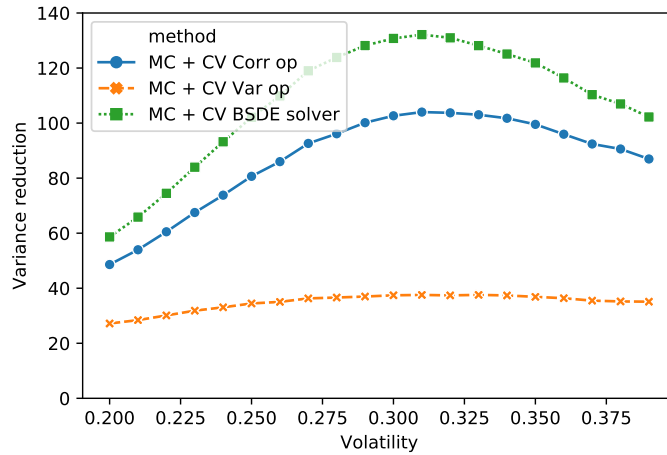


FIGURE 9. Variance reduction with network trained with $\sigma = 0.3$ but applied for $\sigma \in [0.2, 0.4]$ for the model of Example 4.4. We see that the variance reduction factor is considerable even in the case when the network is used with “wrong” σ . It seems that Algorithm 4 is not performing well in this case.

APPENDIX A. MARTINGALE CONTROL VARIATE

Let $(\Omega, \mathcal{F}, \mathbb{P})$ be a probability space and consider an $\mathbb{R}^{d'}$ -valued Wiener process $W = (W^j)_{j=1}^{d'}$ with $(W_t^j)_{t \geq 0}$ for $j=1, \dots, d'$. We will use $(\mathcal{F}_t^W)_{t \geq 0}$ to denote the filtration generated by W . Consider a $D \subseteq \mathbb{R}^d$ -valued, continuous, stochastic process defined for the parameters $\beta \in B \subseteq \mathbb{R}^p$, $X^\beta = (X^{\beta, i})_{i=1}^d = ((X_t^{\beta, i})_{t \geq 0})_{i=1}^d$ adapted to $(\mathcal{F}_t^W)_{t \geq 0}$.

Let $g : C([0, T], \mathbb{R}^d) \rightarrow \mathbb{R}$ be a measurable function. We shall consider path-dependent contingent claims of the form $g((X_s^\beta)_{s \in [0, T]})$. Finally we assume that there is a (stochastic) discount factor given by

$$D(t_1, t_2; \beta) = e^{-\int_{t_1}^{t_2} c(s, X_s^\beta; \beta) ds}$$

for an appropriate function $c = c(t, x; \beta)$. We will omit the β from the discount factor notation. Let

$$\Xi_T^\beta := D(t, T)g((X_s^\beta)_{s \in [0, T]}).$$

We now interpret \mathbb{P} as some risk-neutral measure and so the \mathbb{P} -price of our contingent claim is

$$V_t^\beta = \mathbb{E} \left[\Xi_T^\beta | \mathcal{F}_t^\beta \right] = \mathbb{E} \left[D(t, T)g((X_s^\beta)_{s \in [0, T]}) | \mathcal{F}_t^\beta \right].$$

By assumption Ξ_T^β is \mathcal{F}_T^W measurable and $\mathbb{E}[|\Xi_T^\beta|^2] < \infty$. Hence, from the Martingale Representation Theorem, see e.g. [11, Th. 14.5.1], there exists a unique process $(Z_t^\beta)_t$ adapted to $(\mathcal{F}_t^W)_t$ with $\mathbb{E}[\int_0^T |Z_s^\beta|^2 ds] < \infty$ such that

$$\Xi_T^\beta = \mathbb{E}[\Xi_T^\beta | \mathcal{F}_0^W] + \int_0^T Z_s^\beta dW_s. \quad (13)$$

The proof of the existence of the process $(Z_t^\beta)_t$, is non-constructive. In the setup of the paper, we used the Markovian property of Ξ_t^β to approximate Z_t^β via the associated linear PDE. In the more general non-Markovian setup, [12] provides a numerical method to construct the martingale representation.

Observe that in our setup, $\mathcal{F}_0 = \mathcal{F}_0^W$, $\mathcal{F}_t^\beta \subseteq \mathcal{F}_t^W$ for $t \geq 0$. Hence tower property of the conditional expectation implies that

$$\mathbb{E}[\Xi_T^\beta | \mathcal{F}_t^\beta] = \mathbb{E}[\Xi_T^\beta | \mathcal{F}_0^W] + \int_0^t Z_s^\beta dW_s. \quad (14)$$

Consequently (13) and (14) imply

$$\mathbb{E}[\Xi_T^\beta | \mathcal{F}_t^\beta] = \Xi_T^\beta - \int_t^T Z_s^\beta dW_s.$$

We then observe that

$$V_t^\beta = \mathbb{E}[\Xi_T^\beta | \mathcal{F}_t^\beta] = \mathbb{E} \left[\Xi_T^\beta - \int_t^T Z_s^\beta dW_s \middle| \mathcal{F}_t^\beta \right].$$

If we can generate iid $(W^i)_{i=1}^N$ and $(Z^{\beta, i})_{i=1}^N$ with the same distributions as W and Z respectively then we can consider the following Monte-Carlo estimator of V_t^β :

$$\mathcal{V}_t^{\beta, N} := \frac{1}{N} \sum_{i=1}^N \left(\Xi_T^{\beta, i} - \int_t^T Z_s^{\beta, i} dW_s^i \right).$$

In the companion paper [45] we provide deep learning algorithms to price path-dependent options in the risk neutral measure by solving the corresponding path-dependent PDE, using a combination of Recurrent Neural networks and path signatures to parametrise the process Z^β .

APPENDIX B. MARTINGALE CONTROL VARIATE DEEP SOLVERS

B.1. Empirical correlation maximisation. This method is based on the idea that since we are looking for a good control variate we should directly train the network to maximise the variance reduction between the vanilla Monte-Carlo estimator and the control variates Monte-Carlo estimator by also trying to optimise λ .

Recall we denote $\Xi_T = D(t, T)g((X_s)_{s \in [t, T]})$. We also denote as $M_{t, T}$ as the stochastic integral that arises in the martingale representation of Ξ_T . The optimal coefficient $\lambda^{*, \theta}$ that minimises the variance $\text{Var}[\Xi_T - \lambda M_{t, T}^\theta]$ is

$$\lambda^{*, \theta} = \frac{\text{Cov}[\Xi_T, M_{t, T}^\theta]}{\text{Var}[M_{t, T}^\theta]}.$$

Let $\rho^{\Xi_T, M_{t, T}^\theta}$ denote the Pearson correlation coefficient between Ξ_T and $M_{t, T}^\theta$ i.e.

$$\rho^{\Xi_T, M_{t, T}^\theta} = \frac{\text{Cov}(\Xi_T, M_{t, T}^\theta)}{\sqrt{\text{Var}[\Xi_T] \text{Var}[M_{t, T}^\theta]}}.$$

With the optimal λ^* we then have that the variance reduction obtained from the control variate is

$$\frac{\text{Var}[\mathcal{V}_{t, T}^{\pi, \theta, \lambda^*, N}]}{\text{Var}[\Xi_T]} = 1 - \left(\rho^{\Xi_T, M_{t, T}^\theta} \right)^2.$$

See [17, Ch. 4.1] for more details. Therefore we set the learning task as:

$$\theta^{*, \text{cor}} := \arg \min_{\theta} \left[1 - \left(\rho^{\Xi_T, M_{t, T}^\theta} \right)^2 \right].$$

The implementable version requires the definition of $\mathcal{V}_{t, T}^{\beta, \pi, \theta, \lambda, N}$ in (9), where we set

$$\begin{aligned} \Xi_T^{\beta, \pi, i} &:= D^\pi(t, T)^i g(X_T^{\beta, \pi, i}) \\ M_{t, T}^{\beta, \pi, i, \theta} &:= \sum_{k=1}^{N_{\text{steps}}-1} (D^\pi(t, t_k))^i \mathcal{R}[\partial_x v]_\theta(t_k, X_{t_k}^{\beta, \pi, i}) \sigma(t_k, X_{t_k}^{\beta, \pi, i}) (W_{t_{k+1}}^i - W_{t_k}^i) \end{aligned}$$

The full method is stated as Algorithm 5.

Algorithm 5 Martingale control variates solver: Empirical correlation maximization

Initialisation: θ, N_{tm}

for $i : 1 : N_{\text{tm}}$ **do**

 generate samples $(x_t^{\beta, \pi, i})_{t \in \pi}$ by using numerical SDE solver on (2) and sampling from the distribution of β .

end for

Find $\theta^{*, N_{\text{tm}}}$ using SGD where

$$\theta^{*, N_{\text{tm}}} := \arg \min_{\theta} \left[1 - \left(\frac{\text{Cov}^{N_{\text{tm}}}(\Xi_T^{\beta, \pi})}{\sqrt{\text{Var}^{N_{\text{tm}}}[\Xi_T^{\beta, \pi}] \text{Var}^{N_{\text{tm}}}[M_{t, T}^{\beta, \pi, \theta}]}} \right)^2 \right],$$

where $\text{Var}^{N_{\text{tm}}}, \text{Cov}^{N_{\text{tm}}}$ denote the empirical variance and covariance.

return $\theta^{*, N_{\text{tm}}}$.

APPENDIX C. ARTIFICIAL NEURAL NETWORKS

We fix a locally Lipschitz function $\mathbf{a} : \mathbb{R} \rightarrow \mathbb{R}$ and for $d \in \mathbb{N}$ define $\mathbf{A}_d : \mathbb{R}^d \rightarrow \mathbb{R}^d$ as the function given, for $x = (x_1, \dots, x_d)$ by $\mathbf{A}_d(x) = (\mathbf{a}(x_1), \dots, \mathbf{a}(x_d))$. We fix $L \in \mathbb{N}$ (the number of layers), $l_k \in \mathbb{N}$, $k = 0, 1, \dots, L-1$ (the size of input to layer k) and $l_L \in \mathbb{N}$ (the size of the network output). A fully connected artificial neural network is then given by $\Phi = ((W_1, B_1), \dots, (W_L, B_L))$, where, for $k = 1, \dots, L$, we have real $l_{k-1} \times l_k$ matrices W_k and real l_k dimensional vectors B_k .

The artificial neural network defines a function $\mathcal{R}_\Phi : \mathbb{R}^{l_0} \rightarrow \mathbb{R}^{l_L}$ given recursively, for $x_0 \in \mathbb{R}^{l_0}$, by

$$\mathcal{R}_\Phi(x_0) = W_L x_{L-1} + B_L, \quad x_k = \mathbf{A}_{l_k}(W_k x_{k-1} + B_k), \quad k = 1, \dots, L-1.$$

We can also define the function \mathcal{P} which counts the number of parameters as

$$\mathcal{P}(\Phi) = \sum_{k=1}^L (l_{k-1} l_k + l_k).$$

We will call such class of fully connected artificial neural networks \mathcal{DN} . Note that since the activation functions and architecture are fixed the learning task entails finding the optimal $\Phi \in \mathbb{R}^{\mathcal{P}(\Phi)}$.

APPENDIX D. ADDITIONAL NUMERICAL RESULTS

Example D.1 (Low dimensional basket option). We consider the basket options problem of pricing, using the example from [5, Sec 4.2.3]. The payoff function is

$$g(S) := \max \left(0, \sum_{i=1}^d S^i - K \right).$$

We first consider the basket options problem on two assets, with $d = 2$, $S_0^i = 70$, $r = 50\%$, $\sigma^i = 100\%$, $\Sigma^{ii} = 1$, $\Sigma^{ij} = 0$ for $i \neq j$, and constant strike $K = \sum_{i=1}^d S_0^i$. In line with the example from [5, Sec 4.2.3] for comparison purposes we organise the experiment as follows. The control variates on 20 000 batches of 5 000 samples each of $(s_{t_n}^i)_{n=0}^{N_{\text{steps}}}$ by simulating the SDE 12, where $N_{\text{steps}} = 50$. The assets' initial values s_{t_0} are always constant $S_{t_0}^i = 0.7$. We follow the evaluation framework to evaluate the model, simulating $N_{\text{MC}} \cdot N_{\text{in}}$ paths by simulating 12 with constant $S_0^i = 0.7$ for $i = 1, \dots, 100$. We have the following results:

- i) Table 5 provides the empirical variances calculated over 10^6 generated Monte Carlo samples and their corresponding control variates. The variance reduction measure indicates the quality of each control variate method. Table 5 also provides the cost of training for each method, given by the number of optimiser iterations performed before hitting the stopping criteria, defined defined before with $\epsilon = 5 \times 10^{-6}$.
- ii) Table 6 provides the confidence interval for the variance of the Monte Carlo estimator, and the Monte Carlo estimator with control variate assuming these are calculated on 10^6 random paths.
- iii) Figures 10 and 11 study the iterative training for the BSDE solver. We train the same model four times for different values of ϵ between 0.01 and 5×10^{-6} and we study the number of iterations necessary to meet the stopping criteria defined by ϵ , the variance reduction once the stopping criteria is met, and the relationship between the number of iterations and the variance reduction. Note that the variance reduction stabilises for $\epsilon < 10^{-5}$. Furthermore, the number of training iterations increases exponentially as ϵ decreases. We choose $\epsilon = 5 \times 10^{-6}$.

We note that in the example from [5, Sec 4.2.3], the control variate is trained with $S_0 = 0.7$ fixed. Using this setting, Algorithm 2 cannot be used to approximate the control variate in (9): since the network at $t = 0$, $\mathcal{R}[v]_{\eta_0}$, is trained only at $S_0 = 0.7$, then

automatic differentiation to approximate $\partial_x \mathcal{R}[v]_{\eta_0}$ (0.7) will yield a bad approximation of $\partial_x v(0.7)$; indeed, during training $\mathcal{R}[v]_{\eta_0}$ is unable to capture how v changes around S_0 at $t = 0$. For this reason, Algorithm 2 is not included in the following results.

Method	Emp. Var.	Var. Red. Fact.	Train. Paths	Optimizer steps
Monte Carlo	1.39	-	-	-
Algorithm 3	1.13×10^{-3}	1219	8×10^7	16 129
Algorithm 4	1.13×10^{-3}	1228	3×10^7	6 601
Algorithm 5	1.29×10^{-3}	1076	4×10^7	8 035

TABLE 5. Results on basket options problem on two assets, Example D.1. Models trained with S_0 fixed, non-random. Empirical Variance and variance reduction factor are presented.

Method	Confidence Interval Variance	Confidence Interval Estimator
Monte Carlo	$[4.49 \times 10^{-5}, 1.19 \times 10^{-4}]$	[0.665, 0.671]
Monte Carlo + antithetic paths	$[1.43 \times 10^{-5}, 2.51 \times 10^{-5}]$	[0.667, 0.670]
Algorithm 3	$[2.1329 \times 10^{-8}, 5.6610 \times 10^{-8}]$	[0.6696, 0.6697]
Algorithm 4	$[1.687 \times 10^{-8}, 4.47 \times 10^{-7}]$	[0.6695, 0.6697]
Algorithm 5	$[1.746 \times 10^{-8}, 4.63 \times 10^{-8}]$	[0.6695, 0.6697]

TABLE 6. Results on basket options problem on two assets, Example D.1. Models trained with S_0 fixed, non-random.

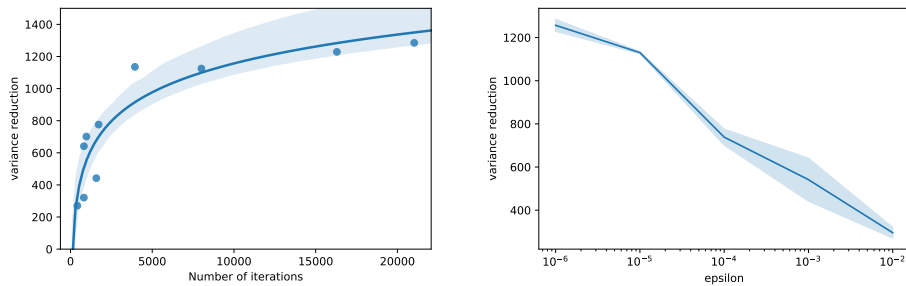


FIGURE 10. Left: Variance reduction in terms of number of optimiser iterations. Right: Variance reduction in terms of epsilon. Both refer to Algorithm 3 used in Example D.1.

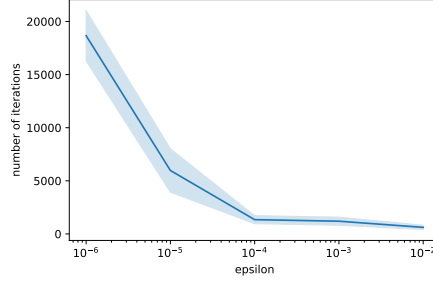


FIGURE 11. Number of optimiser iterations in terms of ϵ for Algorithm 3 used in Example D.1.

Example D.2 (basket option with random sigma). In this example, as in Example 4.2, we aim to show how our approach - where we build a control variate by approximating the process $(Z_{t_k})_{k=0, \dots, N_{\text{steps}}}$ - is more robust compared to directly approximating the price by a certain function in a high-dimensional setting.

We use the methodology proposed in [7], where the authors present a deep learning-based calibration method proposing a two-steps approach: first the authors learn the model that approximates the pricing map using a artificial neural network in which the inputs are the parameters of the volatility model. Second the authors calibrate the learned model using available data by means of different optimisation methods.

For a fair comparison between our deep learning based control variate approach vs. the method proposed in [7], we make the following remarks:

- i) We will only use the the first step detailed in [7] where the input to the model that approximates the pricing map are the volatility model's parameters: $\sigma \in \mathbb{R}^d, r$, and the initial price is considered constant for training purposes. We run the experiment for $d = 5$.
- ii) In [7] the authors build a training set, and then perform gradient descent-based optimisation on the training set for a number of epochs. This is somewhat a limiting factor in the current setting where one can have as much data as they want since it is generated from some given distributions. In line with our experiments, instead of building a training set, in each optimisation step we sample a batch from the given distributions.
- iii) In [7], the price mapping function is learned for a grid of combinations of maturities and strikes. In this experiment, we reduce the grid to just one point considering $T = 0.5, K = \sum_i S_0^i$, where $S_0^i = 0.7 \forall i$.
- iv) We will use Algorithm 3 to build the control variate with the difference that now $\sigma \in \mathbb{R}^d, r \in \mathbb{R}$ will be passed as input to the each network at each time step $\mathcal{R}[v]_{\eta_k}, \mathcal{R}[\partial_x v]_{\theta_k}$.

The experiment is organised as follows:

- i) We train the network proposed in [7] approximating the price using Black-Scholes model and Basket options payoff. In each optimisation iteration a batch of size 1 000, where the volatility model's parameters are sampled using $\sigma \sim \mathcal{U}(0.9, 1.1)$ and $r \sim \mathcal{U}(0.4, 0.6)$. We keep a test set of size 150, $\mathcal{S} = \{[(\sigma^i, r^i); p(\sigma^i, r^i)], i = 1, \dots, 150\}$ where $p(\sigma^i, r^i)$ denotes the price and is generated using 50 000 Monte Carlo samples.
- ii) We use Algorithm 3 to build the control variate, where σ and r are sampled as above and are included as inputs to the network. We denote the trained model by $\mathcal{R}[\partial_x v]_{\theta_k}$ where $k = 1, \dots, N_{\text{steps}}$. In contrast with Algorithm 3.

We present the following results:

- i) Figure 1 displays the histogram of the squared error of the approximation of the PDE solution $\mathcal{R}[v]_\eta$ for each instance in \mathcal{S} . In this sample, it spans from almost 10^{-8} to 10^{-3} , i.e. for almost five orders of magnitude.
- ii) We build the control variate for that instance in the test set for which $\mathcal{R}[v]_\eta$ generalises the worst. For those particular σ, r , Table 7 provides its variance reduction factor.

Method	Emp. Var.	Var. Red. Fact.
Monte Carlo	1.29	-
Algorithm 3	0.035	37

TABLE 7. Results on basket options problem on 5 assets, Model trained with non-random S_0 , and random σ, r .

Example D.3 (High dimensional basket option). We also consider the basket options problem on $d = 100$ assets but otherwise identical to the setting of Example D.1. We compare our results against the same experiment in [5, Sec 4.2.3, Table 6 and Table 7].

Method	Emp. Var.	Var. Red. Fact.	Train. Paths	Opt. Steps
Monte Carlo	79.83	-	-	-
Algorithm 3	4.72×10^{-4}	168 952	24×10^7	47369
Algorithm 4	1.79×10^{-4}	349 525	37×10^6	7383
Algorithm 5	1.54×10^{-4}	517 201	35×10^6	7097
Method ζ_a^1 in [5]	8.67×10^{-1}	97	-	-
Method ζ_a^2 in [5]	4.7×10^{-3}	17 876	-	-

TABLE 8. Results on basket options problem on 100 assets, Example D.3. Models trained with non-random S_0 so that the results can be directly compared to [5].

Table 8 shows a significant improvement of the variance reduction factor (10x and 100x better) of all our Algorithms than the methods proposed in [5] and applied in the same example.

Method	Confidence Interval Variance	Confidence Interval Estimator
Monte Carlo	$[8.57 \times 10^{-4}, 2.27 \times 10^{-3}]$	[27.351, 27.380]
Monte Carlo + antithetic paths	$[5.34 \times 10^{-4}, 9.35 \times 10^{-4}]$	[27.354, 27.371]
Algorithm 3	$[7.001 \times 10^{-9}, 1.8583 \times 10^{-8}]$	[27.3692, 27.3693]
Algorithm 4	$[2.41 \times 10^{-9}, 6.39 \times 10^{-9}]$	[27.36922, 27.36928]
Algorithm 5	$[4.1672 \times 10^{-9}, 1.1060 \times 10^{-8}]$	[27.36922, 27.36928]

TABLE 9. Results on basket options problem on 100 assets, Example D.3. Models trained with non-random S_0 .

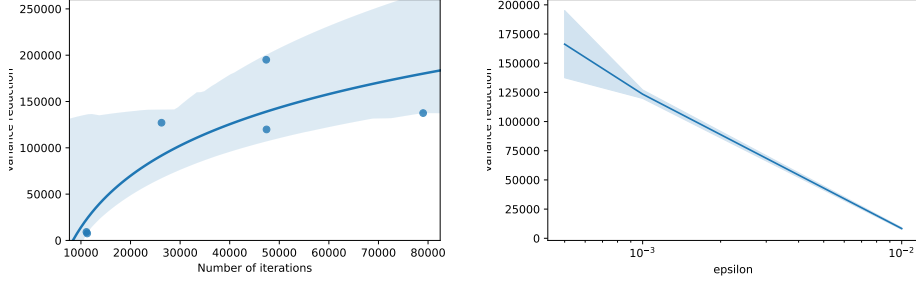


FIGURE 12. Left: Variance reduction in terms of number of optimiser iterations. Right: Variance reduction in terms of epsilon. Both are for Example D.3 and Algorithm 3.

D.1. Empirical network diagnostics. In this subsection we consider the exchange options problem on two assets from Example 4.1, where the time horizon is one day. We consider different network architectures for the BSDE method described by Algorithm 3 in order to understand their impact on the final result and their ability to approximate the solution of the PDE and its gradient. We choose this problem given the existence of an explicit solution that can be used as a benchmark. The experiment is organised as follows:

- i) Let $L - 2$ be the number of hidden layers of $\mathcal{R}[\partial_x v]_{\theta_{t_0}} \in \mathcal{DN}$ and $\mathcal{R}[v]_{\theta_{t_0}} \in \mathcal{DN}$. Let l_k be the number of neurones per hidden layer k .
- ii) We train four times all the possible combinations for $L - 2 \in \{1, 2, 3\}$ and for $l_k \in \{2, 4, 6, \dots, 20\}$ using $\epsilon = 5 \times 10^{-6}$ for the stopping criteria. The assets' initial values $s_{t_0}^i$ are sampled from a lognormal distribution

$$X \sim \exp((\mu - 0.5\sigma^2)\tau + \sigma\sqrt{\tau}\xi),$$

where $\xi \sim N(0, 1)$, $\mu = 0.08$, $\tau = 0.1$.

- iii) We approximate the L^2 -error of $\mathcal{R}[v]_{\theta_{t_0}}(x)$ and $\mathcal{R}[\partial_x v]_{\theta_{t_0}}(x)$ with respect to the exact solution given by Margrabe's formula and its gradient.

Figure 13 displays the average of the L^2 -errors and its confidence interval. We can conclude that for this particular problem, the accuracy of $\mathcal{R}[v]_{\theta_{t_0}}(x)$ does not strongly depend on the number of layers, and that there is no improvement beyond 8 nodes per hidden layer. The training (its inputs and the gradient descent algorithm together with the stopping criteria) becomes the limiting factor. The accuracy of $\mathcal{R}[v]_{\theta_{t_0}}(x)$ is clearly better with two or three hidden layers than with just one. Moreover it seems that there is benefit in taking as many as 10 nodes per hidden layer.

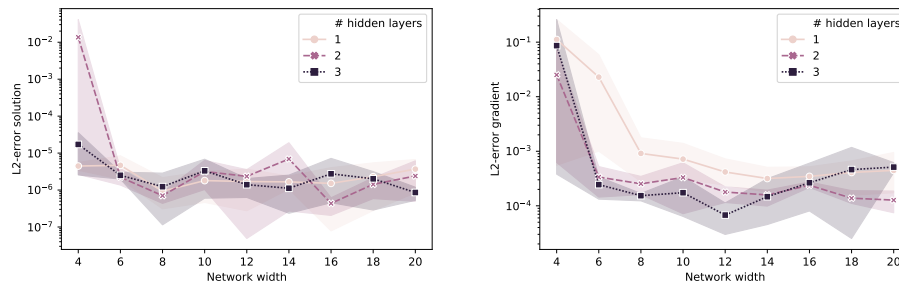


FIGURE 13. Average error of PDE solution approximation and its gradient and 95% confidence interval of different combination of # of layers and net width. Left: error model. Right: Error grad model

ACKNOWLEDGEMENTS

This work was supported by the Alan Turing Institute under EPSRC grant no. EP/N510129/1.

REFERENCES

- [1] C. Bayer and B. Stemper. Deep calibration of rough stochastic volatility models. *arXiv:1810.03399*, 2018.
- [2] C. Beck, S. Becker, P. Grohs, N. Jaafari, and A. Jentzen. Solving stochastic differential equations and kolmogorov equations by means of deep learning. *arXiv:1806.00421*, 2018.
- [3] C. Beck, L. Gonon, and A. Jentzen. Overcoming the curse of dimensionality in the numerical approximation of high-dimensional semilinear elliptic partial differential equations, 2020.
- [4] D. Belomestny, S. Hafner, T. Nagapetyan, and M. Urusov. Variance reduction for discretised diffusions via regression. *Journal of Mathematical Analysis and Applications*, 458(1):393–418, 2018.
- [5] D. Belomestny, L. Iosipoi, and N. Zhivotovskiy. Variance reduction via empirical variance minimization: convergence and complexity. *arXiv:1712.04667*, 2017.
- [6] J. Berner, P. Grohs, and A. Jentzen. Analysis of the generalization error: Empirical risk minimization over deep artificial neural networks overcomes the curse of dimensionality in the numerical approximation of black–scholes partial differential equations. *SIAM Journal on Mathematics of Data Science*, 2(3):631–657, Jan 2020.
- [7] M. T. Blanka Horvath, Aitor Muguruza. Deep learning volatility: A deep neural network perspective on pricing and alibration in (rough) volatility models. *arXiv:1901.09647*, 2019.
- [8] M. Broadie, Y. Du, and C. C. Moallemi. Risk estimation via regression. *Operations Research*, 63(5):1077–1097, 2015.
- [9] Q. Chan-Wai-Nam, J. Mikael, and X. Warin. Machine learning for semi linear pdes. *Journal of Scientific Computing*, 79(3):1667–1712, 2019.
- [10] L. Chizat and F. Bach. On the global convergence of gradient descent for over-parameterized models using optimal transport. In *Advances in neural information processing systems*, pages 3036–3046, 2018.
- [11] S. N. Cohen and R. J. Elliott. *Stochastic calculus and applications*. Springer, 2015.
- [12] R. Cont and Y. Lu. Weak approximation of martingale representations. *Stochastic Processes and their Applications*, 126(3):857–882, Mar 2016.
- [13] J. Cvitanic, J. Zhang, et al. The steepest descent method for forward-backward sdes. *Electronic Journal of Probability*, 10:1468–1495, 2005.
- [14] J. B. Diederik P. Kingma. Adam: A method for stochastic optimization. *arXiv:1412.6980*, 2017.
- [15] S. S. Du, X. Zhai, B. Póczos, and A. Singh. Gradient descent provably optimizes over-parameterized neural networks. *arXiv:1810.02054*, 2018.
- [16] D. Elbrächter, P. Grohs, A. Jentzen, and C. Schwab. Dnn expression rate analysis of high-dimensional pdes: Application to option pricing. *Constructive Approximation*, May 2021.
- [17] P. Glasserman. *Monte Carlo methods in financial engineering*. Springer, 2013.
- [18] L. Gonon, P. Grohs, A. Jentzen, D. Kofler, and D. Šiška. Uniform error estimates for artificial neural network approximations for the heat equation. *IMA Journal Numerical Analysis*, 2021.
- [19] I. Goodfellow, J. Shlens, and C. Szegedy. Explaining and harnessing adversarial examples. *arXiv:1412.6572*, 2014.

- [20] P. Grohs, F. Hornung, A. Jentzen, and P. von Wurstemberger. A proof that artificial neural networks overcome the curse of dimensionality in the numerical approximation of Black-Scholes partial differential equations. *arXiv:1809.02362*, 2018.
- [21] P. Grohs, A. Jentzen, and D. Salimova. Deep neural network approximations for monte carlo algorithms, 2019.
- [22] J. Han, A. Jentzen, et al. Solving high-dimensional partial differential equations using deep learning. *arXiv:1707.02568*, 2017.
- [23] J. Han and J. Long. Convergence of the deep bsde method for coupled fbsdes. *Probability, Uncertainty and Quantitative Risk*, 5(1):1–33, 2020.
- [24] P. Henry-Labordere. Deep primal-dual algorithm for BSDEs: Applications of machine learning to CVA and IM. *Available at SSRN 3071506*, 2017.
- [25] A. Hernandez. Model calibration with neural networks. *Available at SSRN 2812140*, 2016.
- [26] B. Horvath, A. Muguruza, and M. Tomas. Deep learning volatility. *Available at SSRN 3322085*, 2019.
- [27] K. Hu, Z. Ren, D. Šiška, and L. Szpruch. Mean-Field Langevin Dynamics and Energy Landscape of Neural Networks. *Annales de l'Institut Henry Poincaré Probability and Statistics*, 57(4):2043–2065, 2021.
- [28] C. Huré, H. Pham, and X. Warin. Some machine learning schemes for high-dimensional nonlinear PDEs. *arXiv:1902.01599*, 2019.
- [29] M. Hutzenthaler, A. Jentzen, T. Kruse, and T. A. Nguyen. A proof that rectified deep neural networks overcome the curse of dimensionality in the numerical approximation of semilinear heat equations. *SN Partial Differential Equations and Applications*, 1(2), Apr 2020.
- [30] A. Itkin. Deep learning calibration of option pricing models: some pitfalls and solutions. *arXiv:1906.03507*, 2019.
- [31] A. J. Jacquier and M. Oumgari. Deep PPDEs for rough local stochastic volatility. *Available at SSRN 3400035*, 2019.
- [32] A. Jentzen, D. Salimova, and T. Welti. A proof that deep artificial neural networks overcome the curse of dimensionality in the numerical approximation of Kolmogorov partial differential equations with constant diffusion and nonlinear drift coefficients. *arXiv:1809.07321*, 2018.
- [33] N. Krylov. On Kolmogorov's equations for finite dimensional diffusions. In *Stochastic PDE's and Kolmogorov Equations in Infinite Dimensions*, pages 1–63. Springer, 1999.
- [34] N. V. Krylov. *Introduction to the theory of random processes*. American Mathematical Society, 2002.
- [35] G. Kutyniok, P. Petersen, M. Raslan, and R. Schneider. A theoretical analysis of deep neural networks and parametric pdes, 2020.
- [36] Y. LeCun, Y. Bengio, and G. Hinton. Deep learning. *Nature*, 521(7553):436, 2015.
- [37] S. Liu, A. Borovykh, L. A. Grzelak, and C. W. Oosterlee. A neural network-based framework for financial model calibration. *arXiv:1904.10523*, 2019.
- [38] W. A. McGhee. An artificial neural network representation of the SABR stochastic volatility model. *SSRN 3288882*, 2018.
- [39] S. Mei, A. Montanari, and P.-M. Nguyen. A mean field view of the landscape of two-layer neural networks. *Proceedings of the National Academy of Sciences*, 115(33):E7665–E7671, 2018.
- [40] G. Milstein and M. Tretyakov. Solving parabolic stochastic partial differential equations via averaging over characteristics. *Mathematics of computation*, 78(268):2075–2106, 2009.
- [41] N. J. Newton. Variance reduction for simulated diffusions. *SIAM Journal on Applied Mathematics*, 54(6):1780–1805, 1994.
- [42] B. Øksendal. Stochastic differential equations. In *Stochastic differential equations*, pages 65–84. Springer, 2003.
- [43] C. Reisinger and Y. Zhang. Rectified deep neural networks overcome the curse of dimensionality for nonsmooth value functions in zero-sum games of nonlinear stiff systems, 2020.
- [44] G. M. Rotskoff and E. Vanden-Eijnden. Neural networks as interacting particle systems: Asymptotic convexity of the loss landscape and universal scaling of the approximation error. *arXiv:1805.00915*, 2018.
- [45] M. Sabate-Vidales, D. Šiška, and L. Szpruch. Solving path dependent pdes with LSTM networks and path signatures, 2020.
- [46] C. S. Sergey Ioffe. Batch normalization: Accelerating deep network training by reducing internal covariate shift. *arXiv:1502.03167*, 2015.
- [47] J. Sirignano and K. Spiliopoulos. DGM: A deep learning algorithm for solving partial differential equations. *arXiv:1708.07469*, 2017.
- [48] J. Sirignano and K. Spiliopoulos. Mean field analysis of neural networks: A central limit theorem. *Stochastic Processes and their Applications*, 2019.
- [49] H. Stone. Calibrating rough volatility models: a convolutional neural network approach. *arXiv:1812.05315*, 2018.
- [50] Z. Wang and S. Tang. Gradient convergence of deep learning-based numerical methods for bsdes. *Chinese Annals of Mathematics, Series B*, 42(2):199–216, 2021.

- [51] E. Weinan, J. Han, and A. Jentzen. Deep learning-based numerical methods for high-dimensional parabolic partial differential equations and backward stochastic differential equations. *Communications in Mathematics and Statistics*, 5(4):349–380, 2017.